IN-SITU INVESTIGATION OF AGING PROTOCOL EFFECT ON RELATIVE PERMEABILITY MEASUREMENTS USING HIGH THROUGHPUT EXPERIMENTATION METHODS

Matthieu Mascle, Souhail Youssef, Hervé Deschamps, Olga Vizika

IFP Energies nouvelles, 1&4 avenue de Bois-Préau, Rueil-Malmaison, France

This paper was prepared for presentation at the International Symposium of the Society of Core Analysts held in Trondheim, Norway 26-31st August 2018

ABSTRACT

In this study, we have investigated the effect of two aging protocols (static and dynamic) on oil/water relative permeabilities. Experiments were conducted on a set of initially strongly water-wet outcrop sandstone samples (Bentheimer). The same measurements were also conducted on altered samples using the two different aging protocols. Steady-state relative permeabilities were measured using a state of the art experimental setup (CAL-X). The setup is equipped with an X-Ray radiography facility, enabling monitoring of 2D local saturations in real-time and thus giving access to fluid flow paths during the flooding. Aged samples relative permeability curves show clear differences when compared to water-wet relative permeabilities, hence suggesting that the wettability has been effectively altered. However, the two aging protocols were unable to produce the same results. The dynamic aging has led to an inversion of the original relative permeability curves asymmetry, suggesting a strongly oil-wet system, whereas the static aging protocol has altered the wettability to a lesser extent. The differences can be explained by analyzing a 2D saturation map. In the case of dynamic aging we observe a homogeneous distribution of fluid saturation during fractional flow. On the opposite, the static protocol results in heterogeneous flow paths, confirming that this protocol did not alter uniformly the wettability of the sample and generates a patchier mixed-wettability system.

INTRODUCTION

When evaluating the hydrodynamic behavior of hydrocarbon reservoirs for further production forecasts, a wide set of properties are needed to be fully described. These properties include the reservoir geometry (and its heterogeneities), extensive rock and fluids characterization (referred as SCAL and PVT analysis) and the pressure and temperature (P,T) conditions at which the reservoir is operated. At the laboratory scale, the multi-phase flow characterization is classically performed by

conducting two-phase coreflood experiments to measure relative permeabilities and capillary pressure, as a function of water saturation, as well as S_{wi} and $S_{or,w}$ end-points. In this work, these two end-points respectively refer to the initial brine-water saturation left in the rock after the hydrocarbon displacement and to the quantity of hydrocarbon trapped after its displacement by the brine-water. All these properties strongly depend on the pore-scale geometry of the porous media, the fluids properties (at given P,T conditions) and what is generally referred as the Crude Oil - Brine - Rock interactions (COBR) [1, 2].

To be representative, relative permeabilities, capillary pressure and saturation end-points have to be measured at reservoir conditions. Among these conditions, the core wettability has been demonstrated to be a first order parameter that will strongly affect and control the fluids distribution at the pore-scale in the porous media [3, 4]. In practice, original reservoir wettability is rarely preserved due to different core handling operations. Indeed, cores drilling, storage and cleaning, can lead to wettability alteration due to core exposure to different P, T conditions along with contamination by various fluids (drilling fluids, atmospheric air, solvents …) [5]. Therefore, the restoration of the original reservoir wettability is a key issue to have representative SCAL measurements. Ideally, this is performed by aging the cleaned cores with the reservoir crude-oil, at reservoir P,T conditions and at a brine-water saturation S_w as closed as possible to the S_{wi} measured in the reservoir. Previous studies have demonstrated the dependency of the efficiency of the aging process to many parameters such as the crude oil composition, the aging time, the temperature, the fluid distribution and aging protocols [6, 7]. In addition, a major concern in the wettability restoration process is the impossibility to directly compare the restored wettability with the original one. Nevertheless, the impact of the wettability on both steady- or unsteady-state relative permeabilities has been well demonstrated in numerous studies [4, 8].

In this study, we have investigated the effect of two aging protocols (static and dynamic) on oil/water relative permeabilities using small core samples (10 mm in diameter and 20 mm in length) and High Throughput Coreflood Experimentation using CAL-X platform [9]. The use of such small samples allows to reduce coreflood experiment duration from few weeks to few days while respecting Darcy scale. The CAL-X setup is equipped with an X-Ray radiography facility, enabling monitoring of 2D saturation profiles in real-time and thus giving access to fluid flow paths during flooding. This equipment allows conducting steady-state relative permeability measurements typically in one day. In addition, the access to the 2D local saturations has demonstrated its potential for a better interpretation of global measurements [10, 11]. Experiments were conducted on a set of initially strongly water-wet outcrop sandstone samples (Bentheimer cores).

MATERIAL AND METHODS

Rock samples and fluids

Samples used in this work are water-wet outcrop sandstones from a Bentheimer quarry, with porosity ranging from 19% to 21% and permeability ranging from 930 mD to 2500 mD (see Table 1). Samples were cored with a diamond core drill with 1 cm internal diameter and cut to a length of 2 cm. After being cored, all the samples were dried in an oven for at least 48 hours at a temperature of 60 °C.

The crude-oil used for aging has been chosen for its high asphaltenes and resins fractions (11.6% and 25.3% respectively). It is generally admitted that these two oil components are involved in the wettability alteration [6, 12]. The acid/base number is relatively low. From the chemical analysis of this crude-oil and the synthetic brine-water (30 g/l NaCl), polar interactions between the matrix and the polar components of the crude and surface precipitation of the asphaltenes are the two main mechanisms likely to occur during the aging. Acid/base interactions and ion bindings are not expected. All relative permeability measurements were measured using a synthetic brine at 30 g/l NaCl and dodecane.

Aging Protocols

The cores that went through aging were initially fully saturated with a synthetic brine of 30g/l NaCl then centrifuged with the crude-oil to residual water saturation referred as S_{wic}. The cores were centrifuged with a rotational speed of 2000 rev/min. This rotational speed allowed to generate a differential pressure between the inlet and outlet of the cores of 350 mbars. Considering HPMI curve this pressure is sufficient to reach residual brine-water saturation lower than 15%.

In the static protocol (Protocol 1), the core Bent2 at S_{wic} was immerged in the crude-oil and aged at 80°C for three weeks. In the dynamic protocol (Protocol 2), the core Bent3 was mounted at S_{wic} in a Hassler type cell and continually flooded with the crude oil at 80°C for 1 week. The dynamic ageing involves a constant supply of wettability altering components, expecting to alter the wettability of the core in a larger extent than the static protocol.

Table 1: Core-dimension and petrophysical properties of the plugs used in this work.

Plug name	Origin	Core dimensions		Permeability (mD)	Porosity (frac.)	Aging protocol
		Diameter (mm)	Length (mm)			
Bent1	Bentheimer	9.8	19.5	1490	0.23	Water-wet reference (Protocol 0)
Bent2		9.9	21.7	930	0.22	Protocol 1
Bent3		9.9	18.6	2500	0.22	Protocol 2

Steady state relative permeability measurement

Steady-state kr measurements were conducted using the CAL-X set-up that has been recently designed for high throughput coreflood experimentation [9]. It is composed of an X-ray radiography facility, a fully instrumented multi-fluid injection platform and a dedicated X-ray transparent beryllium core holder. The local and averaged saturation S_w is derived from the radiographs, captured every 10 seconds, using Beer-Lambert law for multi-material.

The different aging protocols described above are expected to alter the cores initial wettability from strongly water-wet to an oil-wet or mixed-wet behavior. In this study, this wettability alteration was indirectly evaluated using steady-state (SS) relative permeability measurement. This method has been preferred to the classical methods (i.e. contact angle measurement or spontaneous imbibition curves) because it gives access, using the 2D saturation map, to the phases partitioning in the core for intermediate phase saturations (ranging from S_{wi} to $S_{or,w}$) at transient and steady state. Thus providing access not only to average core wettability (using the kr-curves), but also to the spatial wettability distribution.

After aging, the cores were inserted in the core holder of the experimental set-up. Before conducting the relative permeability measurements, the crude-oil was removed from the samples by flushing first with cyclohexane to avoid asphaltenes precipitation and then with dodecane. The cyclohexane and the dodecane were flushed until differential pressure and phase-saturation stabilization. After being cleaned from the crude-oil, the cores were set to S_{wi}, through a displacement cycle involving a spontaneous water imbibition, a forced imbibition and a forced drainage with the dodecane. The drainage flow-rate was adapted so that comparable S_{wi} values were reached for all the cores allowing an easier kr-curves comparison (especially the k_{rom} values). The kr measurements were conducted starting from this S_{wi} state of saturation.

The SS method involves the simultaneous injection of both fluids at the inlet of the plug while monitoring the differential pressure and the saturation within the core. Starting from S_{wi}, the different points of the curves $k_{rw}(S_w)$ and $k_{rnw}(S_w)$ are obtained by progressively increasing the fractional flow rate f_w (Q_w/Q_{total}) from 0 to 1. When steady-state is reached for a given f_w, the values $k_{rw}(S_w)$ and $k_{rnw}(S_w)$ are easily obtained using Eq.1. This analytical solving assumes the two conditions, negligible capillary effect and laminar flow (i.e. Reynolds number less than 10). Laminar condition is verified since a linear relation between flow rate and pressure drop is respected during mono-phasic injection. The condition of negligible capillary pressure can't be completely verified here, but the uniformity of the 1D saturation profile at steady-state condition suggests a constant capillary pressure along the axis of the core ($dP/dx = 0$); the high permeability of the cores allows us to assume a low capillary pressure. The relative permeabilities

calculated here were not corrected for the capillary pressure but the error was

$$\begin{cases} k_{rw}(S_w) = \dfrac{\mu_w L}{K_a S} * \dfrac{q_w}{\Delta P_w} \\ k_{rnw}(S_w) = \dfrac{\mu_{nw} L}{K_a S} * \dfrac{q_{nw}}{\Delta P_w + P_c} \end{cases} \quad \text{Eq.1}$$

expected to be minor, allowing the kr-curves comparison.

where q_i is the volumetric flow rate of the phase i (m^3/s), K_a is the absolute permeability (m^2), k_{ri} is the relative permeability of the phase i, μ_i is the fluid viscosity (Pa.s), S_i the saturation of the phase i, ΔP_i the differential pressure measure in the phase i, between the outlet and the inlet of the plug (Pa), P_c is the capillary pressure defined as $P_c = P_{nw} - P_w$, L the length of the plug (m) and S the cross section (m^2).

All the relative permeabilities were measured at ambient temperature (T~23°C) and under confinement pressure (P_{conf}=30bars and P_{pore}=5bars). They are fitted using

$$\begin{cases} k_{rw}(S_w) = k_{rwm} {S_w^*}^{n_w} \\ k_{rnw}(S_w) = k_{rnwm}(1 - S_w^*)^{n_{nw}} \\ \text{with } S_w^* = \dfrac{1 - S_{wi}}{1 - S_{wi} - S_{orw}} \end{cases} \quad \text{Eq.2}$$

Corey equations, using Eq.2 and a non-linear least squares regression:

RESULTS AND DISCUSSION

Steady-state relative permeabilities

The SS relative permeabilities measured on the three Bentheimer cores are given in Figure 1. The fitted Corey's parameters are summarized Table 2. The sample absolute permeability K_a (see Table 1) has been used as reference value to compute k_r-curves presented Figure 1. The end-points $S_{or,w}$ reached during the last fractional flow ($f_w = 1$) and the Corey's parameters are compared Figure 2 and Figure 3 for the different aging protocol.

The relative permeabilities measured on the water-wet sample (Figure 1, blue curves) confirm the cores initial strongly water-wet behaviour, accordingly to Craig's rules of thumb [3]. The measurements show:

- High values for the k_{rom} (above 0.5, in fraction).
- Low values for the k_{rwm} (below 0.13 in fraction).
- A crossing point S_{wc} (S_w when $k_{ro} = k_{rw}$) slightly higher than 0.5.

The strong asymmetry observed between the k_{ro} and k_{rw} curves shows that the pressure losses are more important in the water-phase at every saturation. This suggests a strong phase partitioning in the porous media with the trapping of the brine-phase in the small pores (poorly affecting the oil-phase flowing at S_{wi}) and the trapping of the oil-phase in the bigger pores (strongly affecting the water-phase flowing at $S_{or,w}$). These two kr-curves, characterising the two-phase flow when the cores are at their initial wettability, are referred below as the native relative permeabilities.

The kr-curves measured on the core Bent2 (static protocol) show noticeable differences with the native kr-curves (see Figure 1, red curves). The asymmetry between the two k_{ro} and k_{rw} curves has been reduced: the k_{rom} value remains the same at comparable saturation but the k_{rwm} values is increased from 0.10 to 0.26. For any given saturation, the pressure losses in the oil-phase has increased: the kro-curve is now more curved (i.e. it has a greater Corey exponent, indicating a more oil-wet character). In addition, the $S_{or,w}$ value is significantly reduced from 0.43 to 0.25. Both these observations suggest that the two immiscible fluids distribute differently during the two-phase flow (compared to the native case), resulting in different pressure losses and fluids trapping. Although the original wettability has been altered, the kr-curves do not correspond to a strongly oil-wet system. The initial wettability may have been altered from strongly water-wet to intermediate-wet or mixed-wet as defined by Salathiel [13]. The differentiation between an intermediate or mixed patchy wettability is not possible based on average properties. To get more insight on the nature of wettability alteration, local observations are needed. This can be achieved either using 3D µCT images that can be limited in resolution if large domain has to be imaged or the 2D local saturations that can give access to the dynamic flow pattern of fluids in the porous media during coreflood experiments.

The kr-curves measured on the Bent3 core (altered by applying the dynamic protocol (protocol 2) are also shown in Figure 1 (green curves). Major differences can be observed compared to the native-core curves: the native kr-curves asymmetry has been partially reversed: the k_{rom} value is now lower than the k_{rwm} (0.20 and 0.37 respectively) at comparable S_{wi} and $S_{or,w}$ values. The pressure losses (measured differential pressure) are now more important in the oil-phase than in the water-phase at every saturation. This can be interpreted as a change of the initial phases partitioning in the porous media: the brine-water may now be trapped in the bulk of the biggest pores, affecting the oil-flow at S_{wi} more severely than if the brine was trapped in the smallest pores. Such an inversion of the initial kr-curves asymmetry has been rarely observed in the literature when using the same pair of fluids in an altered system: most of the kr-curves stating a strongly oil-wet system still exhibit k_{rom} value higher than the k_{rwm} [1, 3, 4, 14].

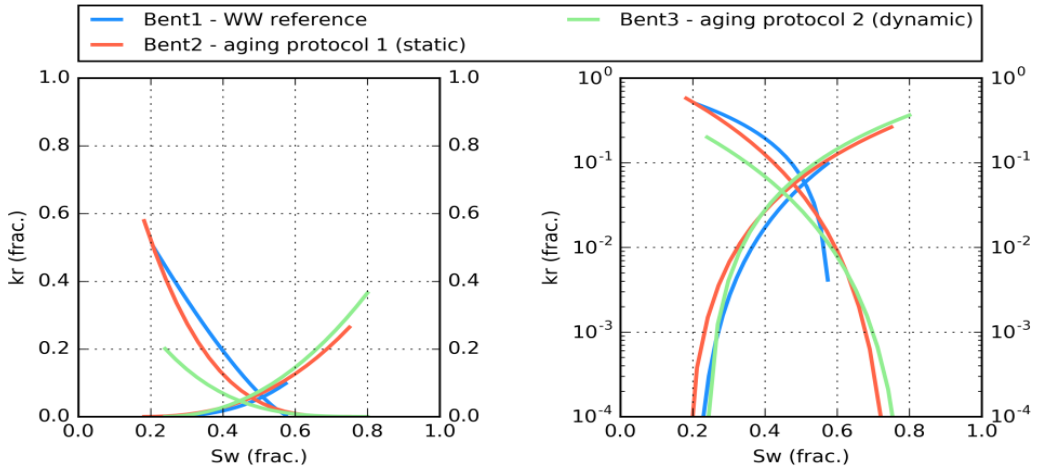

Figure 1: Relative permeabilities normalized with the cores absolute permeabilities *K* (see Table 1). The different curves correspond to the water-wet case (blue curves), the static aging protocol (red curves) and the dynamic aging protocol (green curves).

Table 2: Corey fitted parameters on the measured relative permeabilities, using Eq.2. The subscripts w and o respectively indicate the synthetic brine and the oil (dodecane phase).

Plug name	S_{wi} (frac.)	S_{orw} (frac.)	n_o	n_w	k_{rom}	k_{rwm}
Bent1 (water-wet reference)	0.21	0.43	1.32	2.82	0.50	0.10
Bent2 (static aging)	0.18	0.25	3.23	2.45	0.57	0.26
Bent3 (dynamic aging)	0.24	0.20	3.25	2.13	0.20	0.37

This kr-curves comparison shows that the two aging protocols have both altered the initial core wettability but to a different extent: the dynamic protocol appears to be far more efficient (considering also the reduced aging time for the dynamic protocol). This observation is confirmed by the evolution of residual oil saturation that decreases from 0.43 for the water wet case to 0.2 after the dynamic aging protocol (see Figure 3). The static aging results in an intermediate trapping value of 0.25. S_{wi} on the other hand shows an increasing trend, however a clear conclusion cannot be drawn at this stage, as drainage flow rates were adapted to reach comparable values of initial water saturation.

Figure 3 shows the evolution of the Corey's parameters as the system moves from strongly water-wet to oil-wet (from the left to the right): the asymmetry between the k_{rmax} values and the Corey exponents is inversed from protocol 0 (water-wet reference) to protocol 2 (dynamic aging). As demonstrated in previous work, the crude-oil flooding has a major impact on the wettability alteration [11]. Two mechanisms may be considered: first the destabilisation of the water-films limiting the rock / crude-oil interactions, and second the constant supply of active

components responsible for the wettability alteration (asphaltenes, resins, and other surface active components with polar functional groups).

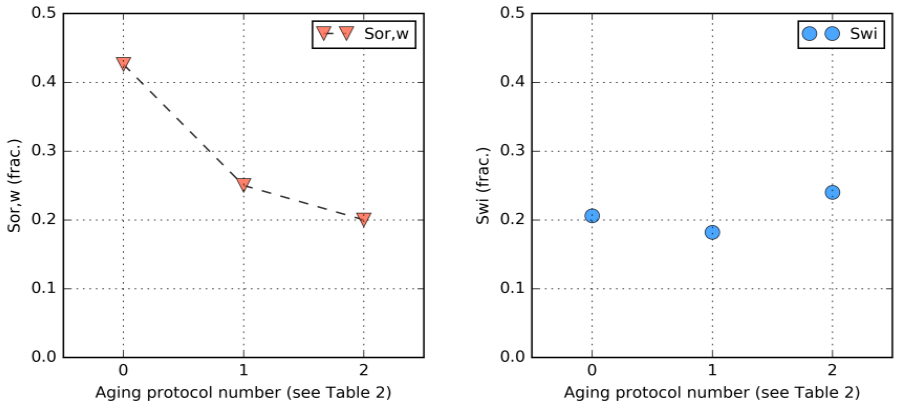

Figure 2: Impact of the aging protocol on the residual oil saturation (S_{orw}) reached at the end of the kr-measurement (fw=1). The S_{wi} values appear slightly impacted as the oil-flushing ($f_w = 0$) was adapted so that comparable values are reached.

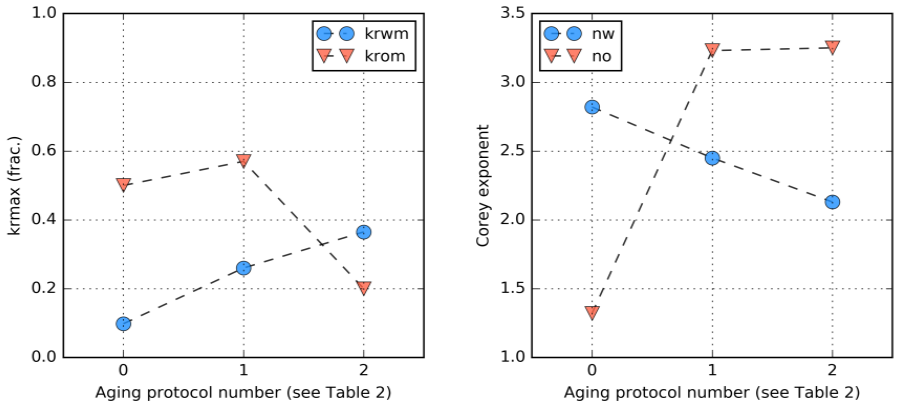

Figure 3: Impact of the aging protocol on the fitted Corey parameters (k_{rmax} on the left and Corey exponent on the right).

2D local saturations

The 2D local saturations imaged during the relative permeability measurements conducted on the two aged cores are given in Figure 5 and Figure 6. A color map is used to draw the phase saturations maps, with hot shades for the 100% oil-phase and cold shades for the 100% brine-phase. Each successive frame (from left to right) is taken at increasing fractional flow f_w, from 0 to 1. The 1D saturation profiles $S_o(X)$ are drawn on each frame to assess the saturation variation along the vertical axis. The spatial resolution of the saturation on the frame is about 0.25 mm.

The 2D saturation map captured on the originate water-wet sample Bent1 shows Figure 4 the uniformity of the saturation when the steady state is reached, in both the vertical and lateral directions, for all frames at the exception of the first frame ($f_w = 0$) that shows a small capillary end-effect. This confirms the hypothesis of constant capillary pressure mentioned above (for $f_w > 0$).

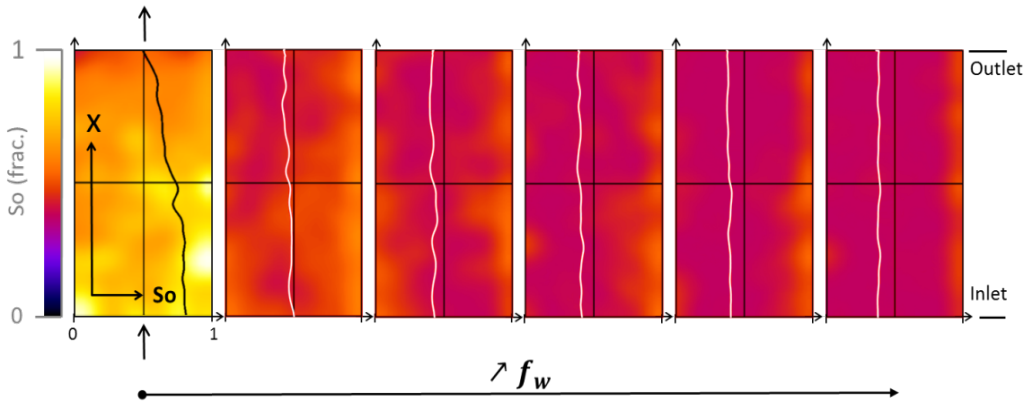

Figure 4: 2D local saturations map during the relative permeabilities measurement conducted on the core Bent1 (water-wet reference). The successive frames are taken at increasing fractional flow f_w from 0 to 1. The 1D saturation along the axis is drawn on each frame.

The 2D saturation maps captured on sample Bent2 (static protocol) reveal a strong heterogeneity on the flow pattern (see Figure 5). The brine-phase is mainly flowing at the center of the core for low and intermediate f_w values. When the water fractional flow is high enough, the flow pattern is fading and the sweeping appears more homogeneous. This heterogeneous flow pattern was also observed during spontaneous imbibition using the synthetic brine (see Figure 7, left) and a spontaneous drainage using the dodecane (see Figure 7, right) conducted on the same core. This was only observed for the core aged with the static protocol. The core aged with the dynamic protocol (Bent3) shows a more homogenous phase partitioning (see Figure 6). The phases partitioning observed during the kr-measurement and the spontaneous displacements on Bent2 can be explained by a spatial heterogeneous wettability alteration (i.e. distinguishable zones with different preferential wettability), with the border of the core being more altered than the center. Similar observations have been made by [11] when altering a chalk sample wettability with a static protocol. Beside the lateral heterogeneity, the frames Figure 5 show a uniformity of the saturation along the vertical axis.

At the end of the experiment, the core Bent2 has been cut along the axis. It shows a pattern of darker areas at the surface of the rock matrix (**Error! Reference source not found.**). This observation can be interpreted as asphaltenes and resin deposits on the porous surface. It should be noted that before being dismounted from the

flowing cell, the cores have been cleaned using Iso-propylic alcohol (IPA) that can potentially remove some of the asphaltenes and resins in the center of the core.

All the results show that the static aging protocol generates a wettability pattern gradient that goes from more oil-wet surface at the border of the sample to more water-wet surfaces at the center of the sample. It is possible that the asphaltene and resin deposits at the border of the core is enhanced by the molecular diffusion of these molecules from the surrounding crude-oil toward the center the core.

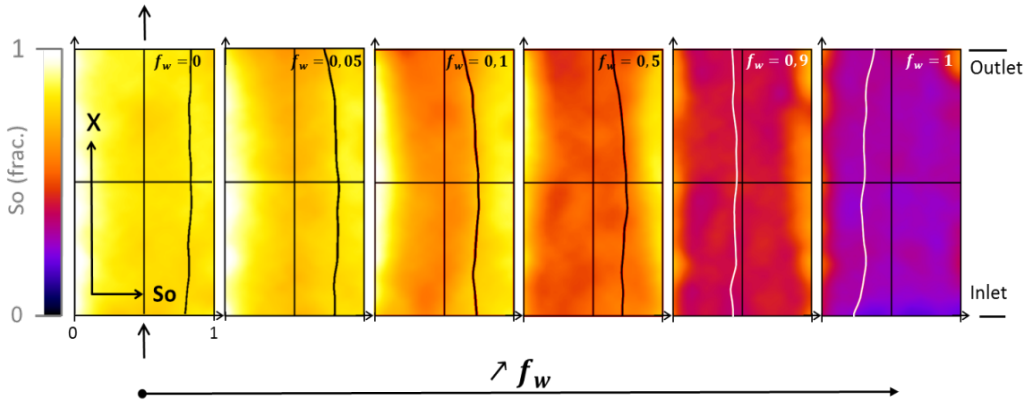

Figure 5: 2D local saturations map during the relative permeabilities measurement conducted on the core Bent2 (static aging). The successive frames are taken at increasing fractional flow f_w from 0 to 1. The 1D saturation along the axis is drawn on each frame.

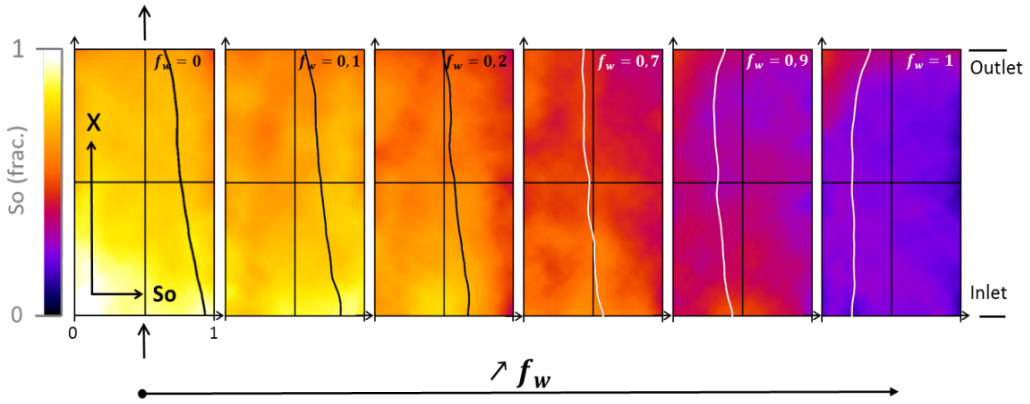

Figure 6: 2D local saturations map during the relative permeabilities measurement conducted on the core Bent3 (dynamic aging). The successive frames are taken at increasing fractional flow f_w from 0 to 1. The 1D saturation along the axis is drawn on each frame.

The 1D saturation profiles measured on the core Bent3 (dynamic ageing) Figure 7 show a non-uniformity of the saturation, with the oil saturation decreasing from the inlet to the outlet of the plug. This heterogeneity may not be explained by a capillary pressure since it was not observed on the core Bent2 (Figure 5). As

mentioned and observed by [10], the unidirectional crude oil flooding during the dynamic ageing can results in a non-uniform wettability alteration with the inlet more altered than the core outlet. This can be explained by a higher pore pressure at the inlet that help thinning the water film and thus the asphaltenes to adsorb on the pores surface.

The 2D insight of the wettability alteration brings valuable information for the interpretation of the core wettability after being aged with the static protocol. The two spontaneous displacements (see Figure 7) suggested a mixed wettability, resulting from the combination of oil-wet and water-wet patches. These results demonstrate the added value of the present method to determine wettability behavior compared to more conventional measurements such as contact angle measurement on model surfaces, underestimating the complexity of the pore space and its impact on the wettability.

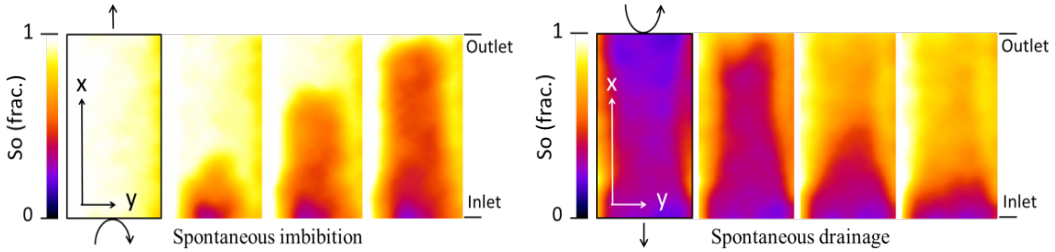

Figure 7: 2D local saturations caught during a spontaneous imbibition with brine (left) and a spontaneous drainage, using the dodecane (right), both conducted on the core Bent2 (static aging).

Figure 8: Along the axis cut of the core Bent2 after treatment following the static aging protocol. The darken areas at the outer part of the core are asphaltene and resin deposits.

CONCLUSIONS

In this work we have presented the impact of two aging protocols on the relative permeability measured using the steady-state method and high throughput experimentation methods. Different wettability alteration patterns have been observed to result from the static and the dynamic aging protocol. The aging has been demonstrated to be more effective when the crude-oil was continuously flooded in the core. A change of the phases partitioning in the porous media has been observed with the dynamic aging, resulting in an inversion of the native kr-curves asymmetry. The 2D local saturation monitoring was shown to bring

valuable information for the core global properties interpretation, providing a tool to confirm assumptions and to qualify non-uniformly distributed properties (e.g. mixed-wettability patterns). It allows demonstrating that the static aging was leading to an incomplete and strongly heterogeneous wettability alteration.

REFERENCES

1. Morrow NR (1990) Wettability and Its Effect on Oil Recovery. Journal of Petroleum Technology 42(12): 1476–1484. doi: 10.2118/21621-PA
2. Cuiec L (1984) Rock/Crude-Oil Interactions and Wettability: An Attempt To Understand Their Interrelation. In: SPE Annual Technical Conference and Exhibition. Society of Petroleum Engineers
3. Craig F. F. (1971) The Reservoir Engineering Aspects Of Waterflooding, SPE Monograph Series Vol. 3. Society of Petroleum Engineers
4. Owens WW, Archer DL (1971) The Effect of Rock Wettability on Oil-Water Relative Permeability Relationships. Journal of Petroleum Technology 23(07): 873–878. doi: 10.2118/3034-PA
5. Anderson WG (1987) Wettability Literature Survey Part 5: The Effects of Wettability on Relative Permeability. Journal of Petroleum Technology 39(11): 1453–1468. doi: 10.2118/16323-PA
6. Buckley JS, Liu Y, Xie X et al. (1997) Asphaltenes and Crude Oil Wetting - The Effect of Oil Composition. SPE Journal 2(02): 107–119. doi: 10.2118/35366-PA
7. Buckley JS, Liu Y, Monsterleet S (1998) Mechanisms of Wetting Alteration by Crude Oils. SPE Journal 3(01): 54–61. doi: 10.2118/37230-PA
8. McCaffery FG, Bennion DW (1974) The Effect OfWettability On Two-Phase Relative Penneabilities. Journal of Canadian Petroleum Technology 13(04). doi: 10.2118/74-04-04
9. Youssef S, Mascle M, Vizika O (2018) High Throughput Coreflood Experimentation as a Tool for EOR Project Design. In: SPE Improved Oil Recovery Conference. Society of Petroleum Engineers
10. Spinler E.A. ,Baldwin B.A. , Graue A. (ed) (1999) Simultaneous measurement of multiple capillary pressure curves from wettability and rock property variations within single rock plugs, SCA9957, Reviewed Proc
11. Graue A, Aspenes E, Bognø T et al. (2002) Alteration of wettability and wettability heterogeneity. Journal of Petroleum Science and Engineering 33(1-3): 3–17. doi: 10.1016/S0920-4105(01)00171-1
12. American Petroleum Institute (ed) (1941) The Effect Of Polar Impurities Upon Capillary And Surface Phenomena In Petroleum Production, API-41-341
13. Salathiel RA (1973) Oil Recovery by Surface Film Drainage In Mixed-Wettability Rocks. Journal of Petroleum Technology 25(10): 1216–1224. doi: 10.2118/4104-PA
14. Donaldson EC, Thomas RD (1971) Microscopic Observations of Oil Displacement in Water-Wet and Oil-Wet Systems. In: Fall Meeting of the Society of Petroleum Engineers of AIME. Society of Petroleum Engineers